applied sciences

MDPI

Article

Research and Application of Coupled Mechanism and Data-Driven Prediction of Blast Furnace Permeability Index

Kangkang Tan [1,2,3,4,5], Zezheng Li [1,2,3,4,5], Yang Han [1,5,*], Xiwei Qi [1,2,3,4,5] and Wei Wang [1,2,3,4,5]

1 Hebei Engineering Research Center for the Intelligentization of Iron Ore Optimization and Ironmaking Raw Materials Preparation Processes, North China University of Science and Technology, Tangshan 063210, China; tankangkang@stu.ncst.edu.cn (K.T.); lizezheng@stu.ncst.edu.cn (Z.L.); qixiwei@ncst.edu.cn (X.Q.); wangwei@stu.ncst.edu.cn (W.W.)
2 Hebei Key Laboratory of Data Science and Application, North China University of Science and Technology, Tangshan 063210, China
3 The Key Laboratory of Engineering Computing, North China University of Science and Technology, Tangshan 063210, China
4 Tangshan Intelligent Industry and Image Processing Technology Innovation Center, North China University of Science and Technology, Tangshan 063210, China
5 College of Metallurgy and Energy, North China University of Science and Technology, Tangshan 063210, China
* Correspondence: hanyang@ncst.edu.cn

Abstract: In order to ensure the stable operation of blast furnace production, it is necessary to keep abreast of the trends in the gas permeability index of the blast furnace. As one of the key parameters to be monitored in the process of blast furnace smelting, the gas permeability index directly reflects the performance of the blast furnace in the actual production of the furnace. Continuous monitoring of the permeability index is required in the actual production of the blast furnace in order to effectively guarantee the stable and smooth operation of the blast furnace. The aim of this study is to accurately predict the trend in the blast furnace gas permeability index by constructing an intelligent prediction model and utilizing a data-driven approach to monitor the gas permeability index and ensure the stable operation of the blast furnace. First, based on the actual production data of a #2 blast furnace of an iron and steel enterprise, an isolated forest algorithm is applied to detect and eliminate the outliers in the original data, and then a data driver set is constructed after normalization of the deviation. Second, by analyzing the coupling mechanism between the blast furnace permeability and gas flow, as well as Spearman correlation analysis and MIC maximum information coefficient (MIC) analysis, key parameters are screened out as feature variables from the data-driven set. Finally, a wavelet neural network algorithm is used to construct an intelligent prediction model of the blast furnace gas permeability index. Compared with a BP neural network (BP), a particle swarm-optimized BP neural network (PSO-BP), and XGBoost, the wavelet neural network shows obvious advantages when the error is controlled in the range of ± 0.1, and the prediction accuracy can reach 95.71%. The model is applied to the actual production of a #2 blast furnace of an iron and steel enterprise, and the results show that the predicted value of the blast furnace permeability index is highly consistent with the actual value of real-time blast furnace production, which verifies its excellent characteristics.

Keywords: blast furnace permeability index; coupling mechanism; data-driven; wavelet neural network

check for updates

Citation: Tan, K.; Li, Z.; Han, Y.; Qi, X.; Wang, W. Research and Application of Coupled Mechanism and Data-Driven Prediction of Blast Furnace Permeability Index. *Appl. Sci.* **2023**, *13*, 9556. https://doi.org/10.3390/app13179556

Academic Editors: Mariola Saternus and Ladislav Socha

Received: 18 May 2023
Revised: 18 August 2023
Accepted: 21 August 2023
Published: 23 August 2023

1. Introduction

Blast furnace ironmaking is a multifaceted melting process characterized by the simultaneous presence of solid, liquid, and gaseous phases, and it is widely considered to be one of the most complex reactors in the field of chemistry and metallurgy [1]. As one of the important parameters of the monitoring index in blast furnace smelting, engineers can intuitively judge the quality of the furnace's running condition through the change law of the permeability index, and they can quickly predict whether there are abnormal blast furnace conditions such as overhanging material, collapsing material, pipeline stroke spraying material, or a sudden drop in the furnace's temperature. They can then make timely adjustments to restore the blast furnace to a running condition [2,3]. Considering the important influence of the gas permeability on blast furnace production, it is necessary to grasp the change rule of the blast furnace gas permeability index in time and to predict it accurately and effectively. In blast furnace production, the blast furnace permeability index is usually determined by calculating the ratio of the difference between the cold air flow into the furnace, the hot air inlet pressure, and the roof pressure. Therefore, in the actual production process, the blast furnace permeability index is usually obtained a posteriori. If an a priori prediction can be made based on the production data, it will play a crucial role in the stable operation of the blast furnace and make corresponding adjustments in response to abnormal furnace conditions easy to apply in time [4,5].

As a complex and critical process, blast furnace smelting is not easy to shut down and cannot be directly accessed for detailed inspection, making it impossible to fully understand its internal mechanism. Facing this challenge, scholars make full use of big data analysis and intelligent algorithms to explore the internal structure and operation mechanism of the blast furnace by collecting actual blast furnace production data. Big data analytics and intelligent algorithms currently have applications in various fields. Alam Zeb et al. [6] applied meta-heuristic algorithms inspired by the collective behaviors of species such as birds, fish, bees, and ants to various areas of software engineering. This study is a guide for researchers to improve the state of the art of current techniques that are commonly used in software engineering with these meta-heuristics. By digging deeper into the actual production data of the blast furnace, it is possible to reveal hidden patterns and correlations, optimize production patterns, and improve efficiency. Vijay Kumar et al. [7] used a deep neural network to predict the silicon content of the molten iron in a blast furnace and developed a real-time model to achieve online prediction and control of the silicon content. The model's Si prediction accuracy is above 95%, with an error in the range of ± 0.1. N. A. Spirin et al. [8] developed an information system for real-time prediction of iron silica content in a blast furnace based on the knowledge of the processes occurring in the furnace and the general laws of transient processes. The model was customized to the blast furnace conditions, taking into account iron ore feedstock and coke composition and properties as well as variations in blast and smelting parameters, and it provides real-time versus 10 h predictions of silicon content. Pourya Azadi et al. [9] used a hybrid kinetic model for the prediction of iron and slag quality indicators in large-scale blast furnaces to predict iron silica content and slag alkalinity during the blast furnace process and to compensate for the shortcomings of mechanical models. Samik Nag et al. [10] investigated the estimation and prediction of blast furnace radial charge distribution on the distribution of ore and coke as well as the distribution of permeability, taking different materials based on different scales of the blast furnace model for experiments. They proposed a method to estimate and predict the distribution of the blast furnace charge, but this method could not give feedback on the change in the permeability index in the blast furnace during its actual operation. Xiaoli Su et al. [11] established a blast furnace permeability prediction model based on an improved multilayer limit-learning machine and wavelet transform and combined partial least squares with the multilayer limit-learning machine algorithm. They eliminated the multicollinearity of the last hidden layer of the multilayer limit-learning machine and improved the prediction accuracy of the model. However, at this stage, the research on blast furnace permeability based on big data analysis and intelligent algorithms is extremely limited and is still in the initial exploration stage.

The aim of this study is to construct a data-driven prediction model to accurately predict the trend in the blast furnace permeability index, so as to ensure the stable operation of the furnace. Taking the actual hourly production data of a steel enterprise's #2 blast furnace in June and July as the basis, the isolated forest algorithm was applied to process the raw data. Through an analysis of the coupling mechanism of blast furnace gas permeability and gas flow, Spearman correlation analysis, and MIC maximum information coefficient analysis of the key parameters for the selection of characteristic variables, a wavelet neural network (WNN) predictive model of the blast furnace gas permeability index was established. The wavelet neural network is based on the introduction of a BP neural network model based on the theory of wavelet transform. It can accurately predict the trend of blast furnace gas permeability, make timely adjustments to the blast furnace production, and ensure the stable and smooth operation of the blast furnace.

The innovative points of this paper are as follows:

(1) Based on the actual hourly production data of a blast furnace of an iron and steel enterprise, the isolated forest algorithm is applied to detect, remove, and retain the outliers in the original data and to construct a data-driven set after the deviation normalization process.
(2) Characteristic variables were established from the data-driven set by analyzing the coupling mechanism between blast furnace gas permeability and gas flow, as well as performing Spearman correlation analysis and MIC maximum information coefficient analysis.
(3) The wavelet neural network algorithm is used to construct an intelligent prediction model of a blast furnace gas permeability index. The wavelet neural network presents obvious advantages when the error is controlled in the range of ± 0.1, and the prediction accuracy can reach 95.71%. It accurately predicts the change trend in the blast furnace gas permeability index, so as to ensure the stable operation of the furnace.

The article is structured as follows: Section 2 describes the isolated forest algorithm as well as departure normalization for data collection and processing. Section 3 describes the coupling mechanism between blast furnace permeability and gas flow. Here, Spearman correlation analysis and MIC maximum information coefficient (MIC) analysis are performed to screen the characteristic variables. Section 4 describes the establishment of the wavelet neural network (WNN) model. Section 5 presents the model comparison evaluation metrics and experimental results. Section 6 summarizes the work of this paper and provides an outlook for the future.

2. Data Collection and Processing

2.1. Data Collection

The data in this paper are derived from the data recorded during the actual hourly production of a steel company's #2 blast furnace in June and July, from which 25 key parameters affecting blast furnace production were selected, and the selection of the off-construction parameters was based mainly on the actual production experience of engineers and a large number of references from the literature [1,7–11]. The data collection was difficult due to the blast furnace production environment. However, it is important to acknowledge that the selection of these critical parameters involves a certain level of subjectivity and may benefit from further refinement and enhancement. Among the selected 25 key parameters, the permeability index serves as the target variable in the prediction model, and the remaining key parameters are considered as the explanatory variables. Table 1 presents the list of 25 selected key parameters.

Table 1. Choosing 25 main variables that affect production process of blast furnace.

Serial Number	key Parameters	Serial Number	Key Parameters	Serial Number	Key Parameters
1	Breathability index	10	Gas CO_2 volume fraction	19	Furnace belly gas volume
2	Furnace top pressure	11	Gas CO volume fraction	20	Iron temperature
3	Differential pressure	12	Gas H_2 volume fraction	21	Furnace belly gas index
4	Gas utilization	13	Gas N_2 volume fraction	22	Northwest furnace body hydrostatic
5	Oxygen enrichment	14	Oxygen enrichment rate	23	Northeast furnace body hydrostatic
6	Wind temperature	15	Cold air flow	24	Southeast furnace body hydrostatic
7	Furnace top temperature	16	Theoretical combustion temperature	25	Southwest furnace body hydrostatic
8	Hot air pressure	17	Blast kinetic energy		
9	Coal injection volume	18	Total load		

2.2. Data Processing

2.2.1. Outlier Handling

Analysis of the data collected at the blast furnace site reveals that there may be many unreasonable outliers in the collected data due to the influence of uncontrollable factors such as the equipment and environment, which must be combined with appropriate data cleaning and rejection methods. Therefore, to handle outliers in the blast furnace data, the following approach was employed:

(1) Outlier detection. There are many ways to detect data outliers. Common methods include 3σ criterion (Lajda criterion) distribution and box plots. The 3σ criterion distribution [12] is a method based on the calculation of the standard deviation, which results in limited processing of the data collected at the blast furnace site, because the data must satisfy a normal distribution. A box plot [13] is essentially a statistical graph used to show the dispersion of data, but it may not provide an accurate assessment of the skewness and tail weight of the data distribution. In addition, for datasets that contain relatively large batches of data, box plots reflect more ambiguous information. Therefore, in this study, an isolated forest algorithm was utilized for detecting anomalies in the blast furnace site data. Isolated forest [14] is a nonparametric machine-learning method that does not require a specific mathematical model to model or label anomalous data, allowing for unsupervised anomaly detection. Its schematic structure is shown in Figure 1.

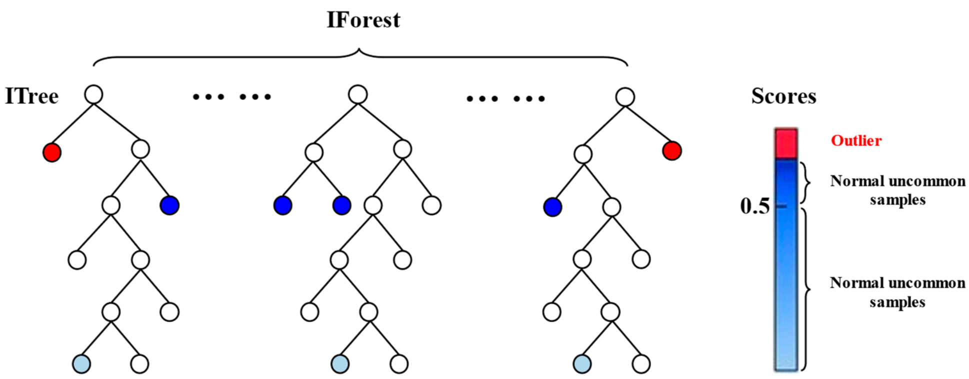

Figure 1. Isolated forest structure graph.

The isolated forest algorithm is used to randomly divide the data interval of the blast furnace site to construct a binary tree. Each leaf node represents a data node. The path length from the leaf node to the root node reflects the degree of dispersion of the data node.

The isolated forest is constructed, and the key is calculated. For the fraction of outliers in the parameters, the specific calculation method is shown in Equations (1)–(3):

$$s(x,n) = 2^{-\frac{E(h(x))}{c(n)}} \tag{1}$$

$$c(n) = \begin{cases} 2H(n-1) - \frac{2(n-1)}{n}, & n > 2 \\ 1, & n = 2 \\ 0, & n < 2 \end{cases} \tag{2}$$

$$H(i) = ln(i) + 0.5772156649 \tag{3}$$

where: $E(h(x))$ denotes the mean value of the path length of the data in the forest; $s(x,n)$ is the anomaly score of node x; $c(n)$ is defined as the mean path length of the search failure in the binomial search tree; $H(i)$ is the number of matching levels, and 0.5772156649 is the Euler constant. The function $s(x,n)$ assigns a higher value to data points that are more likely to be anomalies, and the anomaly data are determined based on a predefined threshold.

(2) Anomaly analysis. The key parameters of the blast furnace are comprehensively analyzed, and abnormal values are studied and judged in combination with the operation mechanism of the blast furnace.

(3) Abnormal value rejection and retention. Abnormal values caused by failures of blast furnace test equipment are rejected; abnormal values resulting from irregular blast furnace operations are retained and considered as part of the analysis.

2.2.2. Normalization Process

In the blast furnace melting process, each key parameter variable has special characteristics, and there are certain differences in the magnitudes and values between each key parameter, which will inevitably affect the output results of the blast furnace permeability prediction. For example, the collected blast furnace data have an oxygen enrichment parameter in the range of [1, 10] and a blast kinetic energy parameter in the range of [8000, 14,000]. As such, the input parameter variables need to be normalized to ensure that some of the data are transformed to the same scale, so that comparisons can be made between the data. In this paper, the data are normalized using the disparity normalization method.

For the data set $X(i) = (x_1, x_2, \ldots, x_n)$, this method employs linear transformation using the maximum and minimum values of the dataset, ensuring that the resulting values are normalized within the range of [0, 1], which is calculated as shown in Equation (4):

$$y_i = \frac{x_i - min(x)}{max(x) - min(x)}, i = 1, 2, \ldots, n \tag{4}$$

where: $max(x)$, $min(x)$ are the maximum and minimum values in the data set, respectively.

2.3. Data Set Creation

After processing the collected data using the above method, the outliers in the 25 parameter variables that were initially selected were manually cleaned and removed. The collected data were consolidated based on time series correlation to create an initial data set for constructing the blast furnace permeability model. The blast furnace permeability index dataset was then randomly divided into two groups: 80% of the data set is used as a training set to train the blast furnace permeability index prediction model. The remaining 20% of the data set is used as a test set to comprehensively evaluate the effect of the blast furnace permeability index prediction model.

3. Data Collection and Processing

The objective of feature parameter selection is to reduce the number of parameters, enhancing the model's generalizability and mitigating the risk of overfitting. The correlation analysis between the target parameter blast furnace air permeability and characteristic parameters is carried out, and the characteristic parameters strongly related to blast furnace air permeability are used as input variables of the data-driven model. In this study, the collected blast furnace production data are analyzed by the nonlinear correlation analysis method. First, the analysis of the interplay between blast furnace permeability and gas flow is used, and second, Spearman correlation analysis and MIC (maximum information coefficient) analysis are selected to correlate the characteristic parameters. Finally, the merged set of analysis results is selected as the input variable.

3.1. Coupling Mechanism Analysis

Blast furnace air permeability is related to the quality of the downstream situation of the blast furnace, as well as the blast furnace smelting strength, energy consumption, and iron quality, is the most critical parameter in the blast furnace, which is determined by the blast furnace smelting process. The blast furnace is a tall, large, and enclosed reactor. It is called a "black box", because its internal closed smelting environment cannot be observed [15]. Its structure is shown in Figure 2.

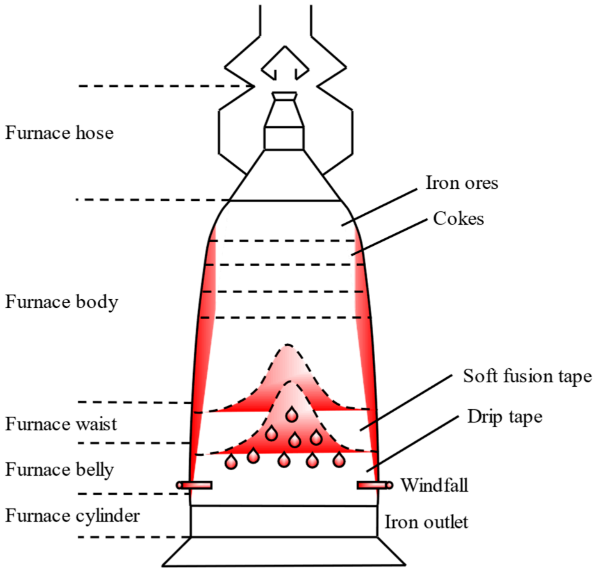

Figure 2. Blast furnace structure.

As the charge descends and the gas stream ascends in synchrony, a sequence of reactions unfolds within the blast furnace:

$$
\begin{array}{ll}
> 570\ ^\circ\mathrm{C} & 3FeO + CO \rightarrow 2FeO + CO + 8870\ \mathrm{kcal} \\
 & 3Fe_2O_3 + CO \rightarrow 2Fe_3O_4 + CO_2 + 8870\ \mathrm{kcal} \\
 & Fe_3O_4 + CO \rightarrow 3FeO + CO_2 - 4990\ \mathrm{kcal} \\
 & FeO + CO \rightarrow Fe + CO_2 + 3250\ \mathrm{kcal} \\
< 570\ ^\circ\mathrm{C} & Fe_3O_4 + 4CO \rightarrow 3Fe + 4CO_2 + 4188\ \mathrm{kcal}
\end{array}
$$

Blast furnace smelting process requirements [16]: These include the furnace charge in the fabric downstream process to maintain a uniform column permeability; blast furnace gas flow in the process of rising, both along the circumferential direction to show a uniform distribution and in the radial direction to have a suitable strong and weak uniform distribution.

3.1.1. Investigation into the Mechanism of Blast Furnace Permeability

Blast furnace permeability denotes the ability of gas to flow within the furnace. It is influenced by various factors, including pore space size, connectivity, and resistance to gas flow within the particle accumulation present in the blast furnace. The formation mechanism of blast furnace permeability is related to the following factors, as shown in Figure 3 [17–19]:

(1) Physical properties of the charge particles: The physical characteristics of the blast furnace charge, including particle size, shape, and surface roughness, impact the interparticle compactness within the blast furnace, consequently influencing its permeability.
(2) Blast furnace operating parameters: The operational variables of the blast furnace encompass factors such as temperature, gas flow rate, and air outlet conditions. These parameters exert a direct influence on the gas flow dynamics and the configuration of particle accumulation within the blast furnace, consequently impacting its permeability.
(3) Charge properties: The mineral composition, bonding characteristics, and other properties of the blast furnace charge play a crucial role in the flowability and discharge behavior of the charge material. Consequently, these properties have a direct impact on the permeability of the blast furnace.
(4) Cylinder structure: The configuration of the blast furnace cylinder also influences the gas flow patterns and the arrangement of particle accumulation within the furnace. These factors, in turn, have an impact on the permeability of the blast furnace.
(5) Furnace dust: There are a large number of furnace dust particles in the blast furnace, and these particles affect the gas flow state and the arrangement of particle accumulation within the blast furnace, subsequently impacting its permeability.

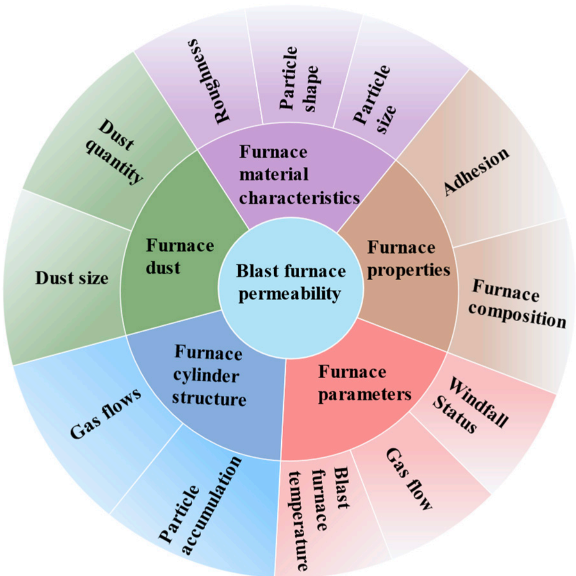

Figure 3. Blast furnace permeability-related factors.

The formation mechanism of blast furnace air permeability is an interrelated and complex issue, which is related to various factors such as physical properties of charge particles, blast furnace operating parameters, charge properties, furnace cylinder structure, and dust in the furnace. Gaining a comprehensive understanding and effectively managing these factors can significantly enhance the air permeability of the blast furnace, thereby ensuring smooth and uninterrupted production.

3.1.2. Analysis of Blast Furnace Gas Flow Mechanism

The formation mechanism of the blast furnace gas flow encompasses various aspects of gas movement within the furnace. Figure 4 illustrates the key influencing factors associated with the gas flow dynamics [20–23]:

(1) Air outlet status: The air outlet status represents a fundamental parameter in blast furnace operation, as it directly determines the speed and direction of gas entry into

the furnace. Consequently, it significantly influences the overall gas flow dynamics within the blast furnace.

(2) Cylinder structure: The configuration of the blast furnace cylinder plays a crucial role in gas flow dynamics. This includes factors such as the shape of the furnace body, the design of the cylinder pipes, and the distribution of slag and iron within the furnace.

(3) Blast furnace charge: The physical and chemical properties of the blast furnace charge, as well as the distribution and arrangement of the charge, will affect the gas flow. For example, parameters such as bonding, humidity, and granularity of the charge will affect the morphology of the particle pile and the gas flow capacity.

(4) Blast furnace parameters: The temperature distribution and pressure conditions within the blast furnace directly impact the gas flow patterns. For instance, the upper section of the furnace experiences higher gas temperatures and lower gas densities, resulting in an upward gas flow, whereas the lower section exhibits a downward gas flow. The flow direction and speed of blast furnace gas are directly affected by the pressure in the furnace.

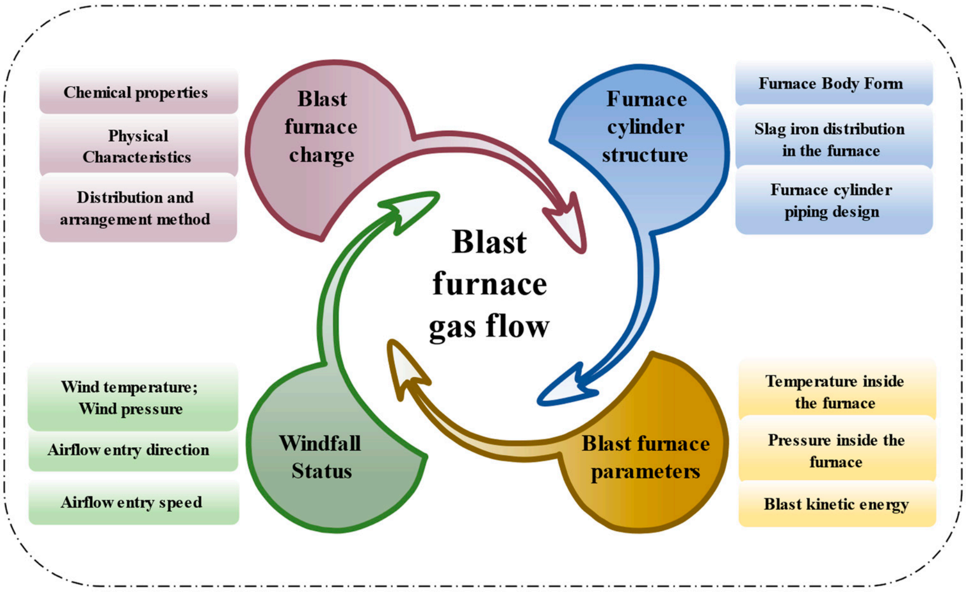

Figure 4. Blast furnace gas flow influence factors.

The formation mechanism of blast furnace gas flow is a complex interplay of multiple factors, including the condition of the air outlet, the structure of the furnace cylinder, the composition of the blast furnace charge, and various parameters such as furnace temperature and pressure. The control of these factors can effectively improve the flow performance of the blast furnace gas stream, thus ensuring the normal production of the blast furnace.

3.1.3. Analysis of the Coupling Mechanism between Blast Furnace Permeability and Gas Flow

The formation mechanism of blast furnace permeability primarily involves the physical and chemical properties of the charge, as well as the distribution and disposition of the charge. The formation mechanism of the blast furnace gas flow involves all aspects of the gas flow in the blast furnace, including the tuyere state, hearth structure, blast furnace charge, furnace temperature, furnace pressure, and other factors. Consequently, there are several interconnected factors between blast furnace permeability and the formation mechanism of blast furnace gas flow [17–23]. First, the permeability of the blast furnace, whether good or poor, significantly impacts the gas flow within it, influencing the speed and direction of the gas movement. Optimal permeability facilitates smooth gas flow, enabling efficient heat and material transfer in the blast furnace and enhancing production efficiency. Conversely, inadequate permeability restricts gas flow speed, impeding heat and material transfer and subsequently reducing the production efficiency of the blast furnace. Second, the direction and speed of blast furnace gas flow also contribute to the formation of blast furnace permeability. Faster gas flow rates facilitate the movement of charge particles, causing the gaps between them to expand and thereby improving blast furnace permeability. Additionally, the direction of gas flow affects permeability. In the upper section of the blast furnace, where gas temperature is higher and gas density is lower, an upward airflow is formed. This upward airflow increases the voids in the upper charge pile, contributing to improved permeability of the blast furnace. Consequently, the formation mechanisms of blast furnace permeability and blast furnace gas flow are inherently interconnected, with each factor influencing the other. Mastering and controlling these mechanisms can improve the production efficiency and product quality of the blast furnace.

3.2. Spearman Correlation Analysis

Spearman correlation analysis [24] discriminates the strength of the correlation by the Spearman rank correlation coefficient; hence, it is also called the Spearman rank correlation coefficient. The principle is to analyze the nonlinear data of 25 critical parameters affecting blast furnace production by solving the ranking position of the original data, ranking the critical parameters ($x_1, x_2, x_3, \ldots, x_{25}$) by the magnitude of the values and establishing the order table, respectively. The position of the order table is called rank order, and the Spearman rank correlation coefficient is calculated as shown in Equation (5):

$$P = 1 - \frac{6\sum_{i=1}^{n}(R_i - Q_i)^2}{n(n^2-1)}, i = 1, 2, \ldots, n \quad (5)$$

where: P is the Spearman rank correlation coefficient; n is the number of variables; R_i and Q_i are the rank order of the two parameter data sets.

A heat map of the Spearman correlation analysis results is shown in Figure 5. The range of the Spearman correlation coefficient is [−1, 1], and the larger the absolute value, the higher the correlation between the two. In general, the absolute value of [0.8, 1] indicates that the correlation between the two is extremely strong; the absolute value of [0.4, 0.8] indicates that the correlation between the two is strong; the absolute value of [0.2, 0.4] indicates that the correlation between the two is weak; the absolute value of [0, 0.2] indicates that the correlation between the two is extremely weak or irrelevant. In this study, key parameters with correlation coefficients greater than 0.3 were selected as data-driven preliminary input variables ($x_2, x_3, x_4, x_6, x_7, x_8, x_{15}, x_{17}$).

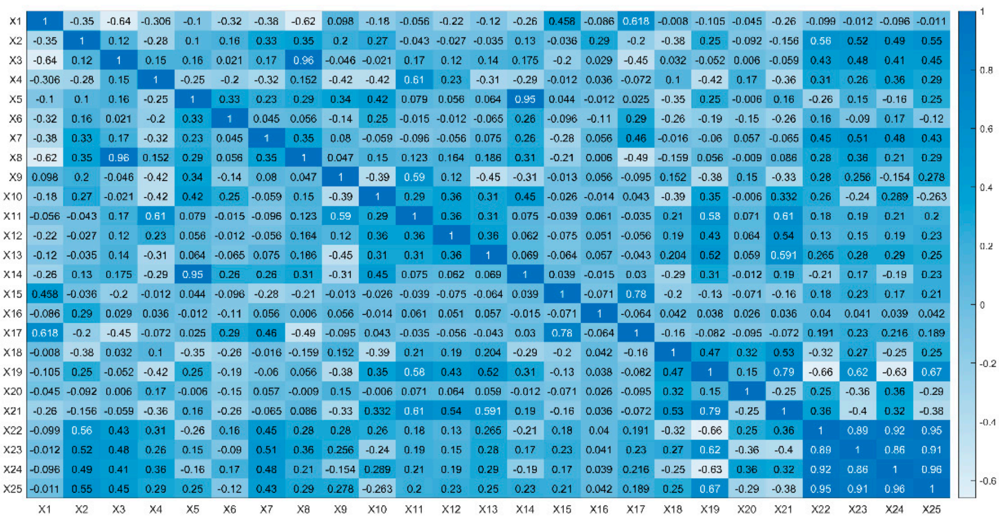

Figure 5. Heat map of Spearman's characteristic correlation analysis.

3.3. MIC Maximum Information Coefficient Analysis

MIC maximum information coefficient analysis [25] is one of the methods to indicate the strength of nonlinear relationships between parameters and is built on the machine-learning concept of feature selection. The larger the MIC, the stronger the association between parameters. The collected data set of 25 critical parameters affecting blast furnace production is analyzed for the MIC, and the blast furnace permeability index is analyzed for the MIC with other critical parameters. Twelve critical parameters ($x_2, x_3, x_4, x_5, x_6, x_7, x_8, x_9, x_{14}, x_{15}, x_{17}, x_{21}$) with MIC coefficients greater than 0.1 were selected, as shown in Figure 6. The specific concept involves selecting a data set consisting of two crucial parameters that are distributed within a two-dimensional space. To analyze this data, an $m * n$ grid is employed to partition the data space and calculate the mutual information of the random variables x and y. The MIC analysis is calculated as shown in Equation (6):

$$MIC(x,y) = \max_{m*n<B} \frac{p(x,y)log_2 \int \frac{p(x,y)}{p(x)p(y)}dxdy}{log_2 min(a,b)} \tag{6}$$

where: m, n denote the number of grid divisions on x, y; $p(x,y)$ denotes the frequency of data points falling in the (x,y) grid; $p(x)$ refers to the frequency of data points falling on the xth row; $p(y)$ refers to the frequency of data points falling on the yth row; and B is the 0.6 power of the data volume.

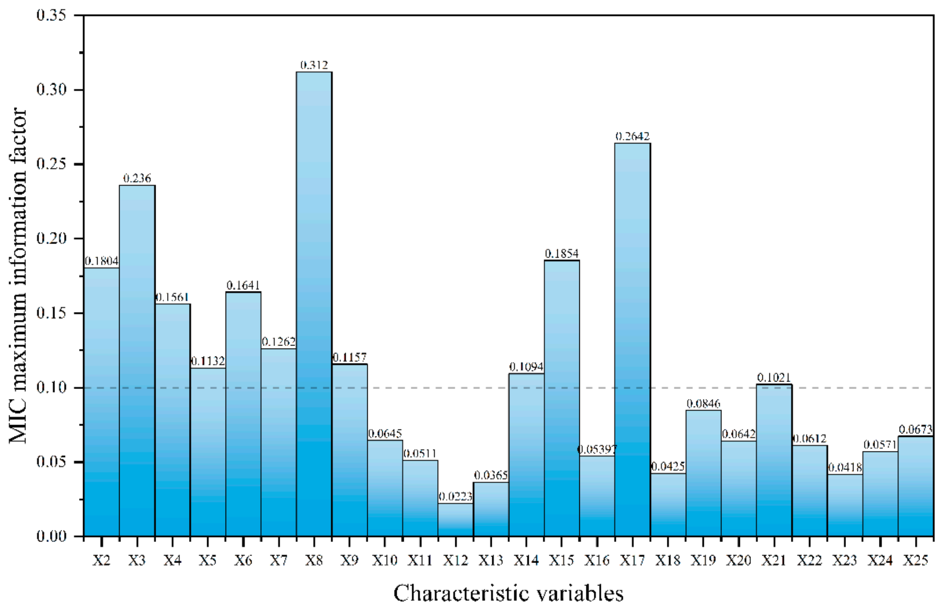

Figure 6. MIC maximum information coefficient.

Establishment of characteristic parameters. Based on the characteristic parameter selection methods of blast furnace permeability and gas flow coupling mechanism analysis, Spearman correlation analysis, and MIC analysis, and summarizing the results of the three analyses and process experience, 14 key parameters were finally selected as the input parameters of the data-driven prediction model. The input parameters are shown in Table 2.

Table 2. Table of prediction model input parameters.

Serial Number	Parameter Name	Serial Number	Parameter Name	Serial Number	Parameter Name
X_2	Furnace top pressure	X_7	Furnace top temperature	X_{14}	Oxygen enrichment rate
X_3	Differential pressure	X_8	Hot air pressure	X_{15}	Cold air flow
X_4	Gas utilization	X_9	Coal injection volume	X_{17}	Blast kinetic energy
X_5	Oxygen enrichment	X_{10}	Gas CO_2 volume fraction	X_{21}	Furnace belly gas index
X_6	Wind temperature	X_{11}	Gas CO volume fraction		

4. Wavelet Neural Network (WNN) Model Building

A wavelet neural network is constructed based on a BP neural network model and wavelet transform theory. It uses a wavelet function instead of an activation function of the hidden layer. It is a new type of backpropagation neural network [26]. The wavelet neural network integrates the time series localization of wavelet transform and the self-learning ability of a neural network, fundamentally solving the problem of localized minima and accelerating the convergence of the network. Its structure is generally divided into three layers: an input layer, a hidden layer, and an output layer. Each layer is passed through the activation function, and there are connection weights. The network structure is shown in Figure 7.

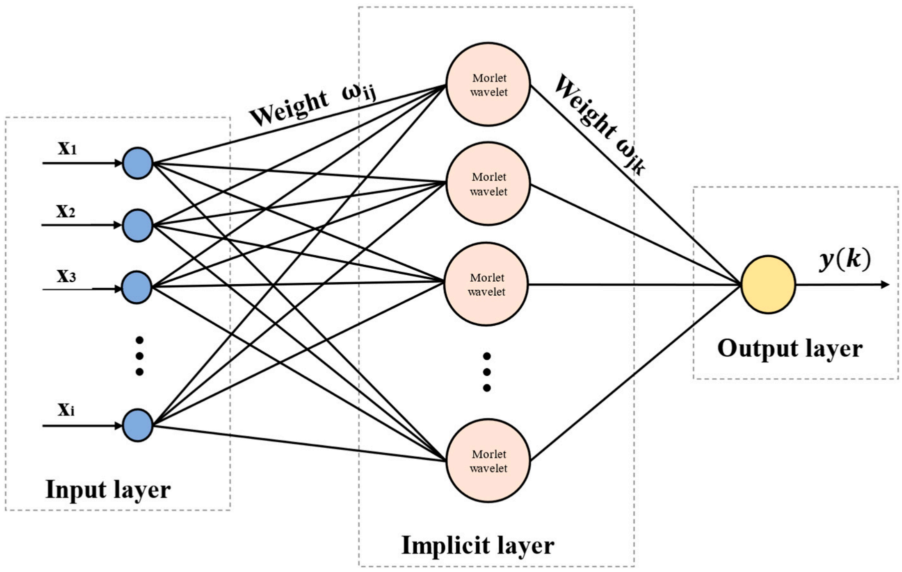

Figure 7. Wavelet neural network structure.

The wavelet basis function of the hidden layer of the wavelet neural network is selected as the Morlet mother wavelet basis function, and the mathematical expression is shown in Equation (7):

$$y = cos\ (1.75x)e^{-x^2/2} \tag{7}$$

An image of the function is shown in Figure 8.

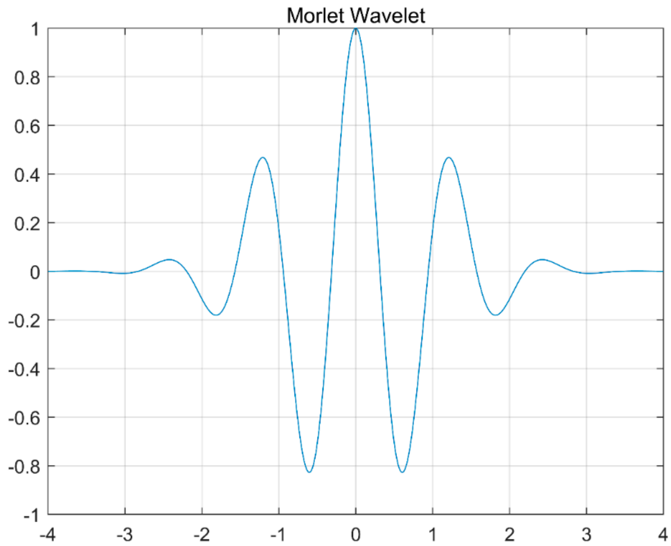

Figure 8. Morlet wavelet function diagram.

The formula for calculating the output of the implicit layer is shown in Equation (8):

$$h(j) = h\left(\frac{\sum_{i=1}^{k} \omega_{ij} x_i - b_j}{a_j}\right),\ j = 1, 2, \ldots l \tag{8}$$

where: x_i is the input value of the wavelet neural network; y is the predicted output value of the wavelet neural network; $h(j)$ is the output value of the jth node in the hidden layer; h is the wavelet basis function; ω_{ij} is the weight of the input layer to the hidden layer; a_j is the scaling factor of the wavelet basis function; and b_j is the translation factor of the wavelet basis function.

The formula for the output layer is shown in Equation (9):

$$y(k) = \sum_{i=1}^{l} \omega_{jk} h(i),\ k = 1, 2, \ldots, m \tag{9}$$

where: ω_{jk} is the weight from the hidden layer to the output layer; l and m are the number of nodes in the hidden layer and the output layer, respectively.

A flow chart of the wavelet neural network prediction steps is shown in Figure 9.

The prediction model for blast furnace permeability, along with the coupling mechanism analysis, enables real-time forecasting of blast furnace permeability. This ensures the continuous operation of the blast furnace and helps prevent any abnormal conditions from occurring. To keep the blast furnace running smoothly, it is necessary to optimize the charge quality and to maintain a normal furnace shape, an active furnace cylinder, adaptable gas distribution, a stable furnace temperature, reasonable slag composition, and good air permeability, etc., among which blast furnace air permeability is especially important. A data-driven blast furnace air permeability prediction model is constructed with 14 parameter variables, including the top pressure, blast kinetic energy, coal injection, differential pressure, cold air flow, belly gas index, gas utilization, hot air pressure, air temperature, top temperature, oxygen enrichment, oxygen enrichment rate, gas CO_2 volume fraction, and gas CO volume fraction. The model's implied layer nodes are set to 14, and the network weight and the learning rate of the wavelet neural network are set to 0.01 and 0.001, respectively.

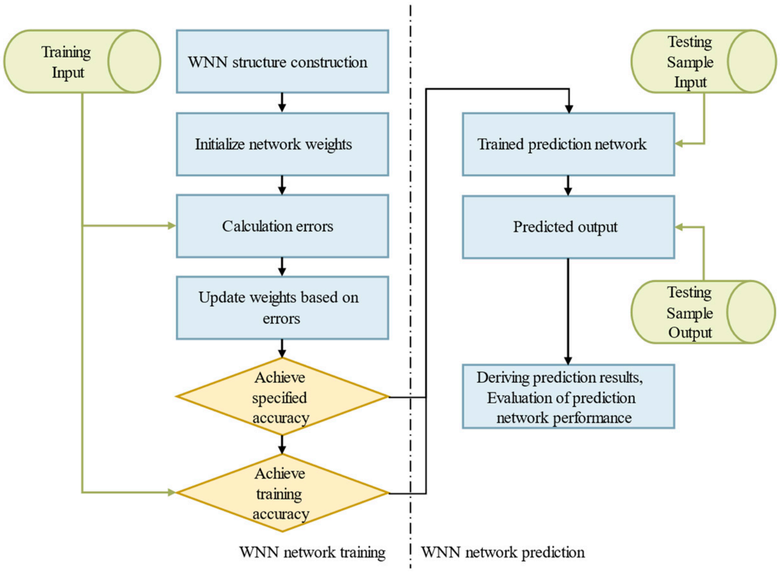

Figure 9. Flow chart of wavelet neural network prediction steps.

5. Research and Application of Prediction Results

The blast furnace permeability index data set selected by feature parameters was sorted by time series, and the wavelet neural network (WNN) was applied for prediction to construct the blast furnace permeability index prediction model. The prediction results are shown in Figure 10. The BP neural network (BP) prediction model, the particle swarm optimization BP neural network (PSO-BP) prediction model, and the Xgboost prediction model were also selected for simulation prediction, and the prediction results obtained were compared with those of the wavelet neural network using evaluation indices.

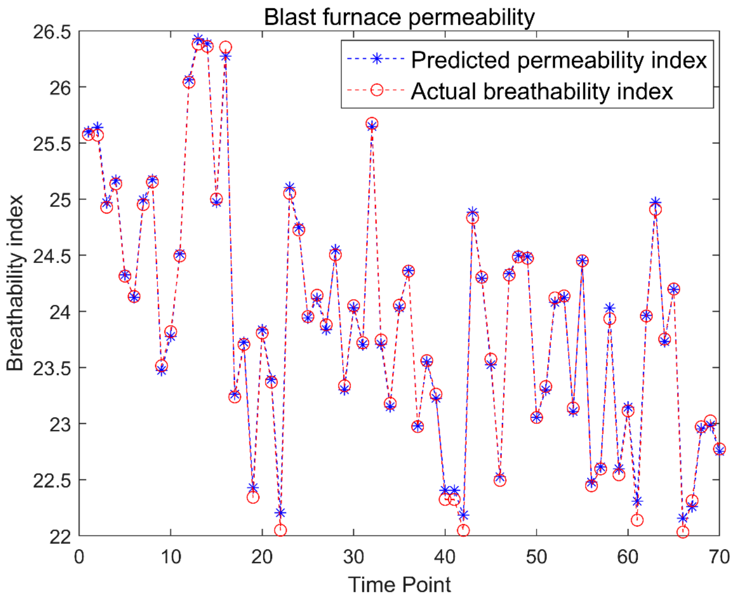

Figure 10. Wavelet neural network model blast furnace permeability index prediction graph.

Upon a thorough analysis of Figure 10, it becomes evident that the prediction results obtained from the wavelet neural network model closely align with the actual values collected. The model demonstrates an impressive accuracy of 95.71% within an error range of ±0.1, making it highly suitable for practical applications in production. Consequently, in this paper, the wavelet neural network model is used to predict the air permeability index of the blast furnace, which can predict the air permeability index of the blast furnace in advance and ensure the smooth operation of the blast furnace.

Four commonly used evaluation indexes, including the RMES (root mean square error), MAE (mean absolute error), MAPE (mean absolute percentage error), and accuracy (model accuracy, error of ±0.1), were selected to compare the performance of the above four prediction models and present an intuitive evaluation of the prediction results. The calculation formulae are shown in Equations (10)–(13) [27]:

$$RMSE = \sqrt{\frac{1}{n}\sum_{i=1}^{n}\left(\hat{y}_i - y_i\right)^2} \tag{10}$$

$$MAE = \frac{1}{n}\sum\nolimits_{i=1}^{n}\left|\hat{y}_i - y_i\right| \tag{11}$$

$$MAPE = \frac{1}{n}\sum\nolimits_{i=1}^{n}\left|\frac{\hat{y}_i - y_i}{y_i}\right| \tag{12}$$

$$ACCURACY = \frac{\dot{n}}{n} \tag{13}$$

where: n denotes the total number of samples; $\hat{y}_i$ denotes the predicted value; y_i denotes the true value; and $\dot{n}$ denotes the number of predicted values within the error allowance.

The RMES, MAE, MAPE, and accuracy of the above four prediction models were calculated based on the blast furnace permeability index simulation prediction results as shown in Table 3.

Table 3. Model performance comparison table.

Name	RMES	MAE	MAPE	Accuracy
BP	0.1527	0.1261	0.5147%	79.89%
PSO-BP	0.1326	0.1107	0.4428%	80.45%
Xgboost	0.1027	0.0871	0.3581%	84.97%
WNN	0.0785	0.0554	0.2347%	95.71%

The comprehensive comparison table above concludes that the wavelet neural network blast furnace permeability index prediction model has the best overall performance and the highest prediction accuracy, and the model accuracy reaches 95.71% at an accuracy error of ±0.1. Therefore, the overall performance of the wavelet neural network in predicting the blast furnace permeability index is better than that of the other three models.

This wavelet neural network blast furnace permeability index prediction model was put into the actual production of a #2 blast furnace in a steel enterprise. The data set of key parameters in a certain time period was collected, the data of the required characteristic parameters were selected for blast furnace permeability index prediction, and the predicted values were compared to the actual production values, as illustrated in Figure 11.

By comparing the predicted values of the blast furnace permeability index with the real-time production values, the efficacy of the prediction algorithm is further validated. The utilization of the prediction model's data in the blast furnace production process enables prompt assessments of the furnace's operational conditions, ensuring its smooth operation. This validation from the perspective of actual blast furnace production confirms the effectiveness of the blast furnace permeability index prediction model.

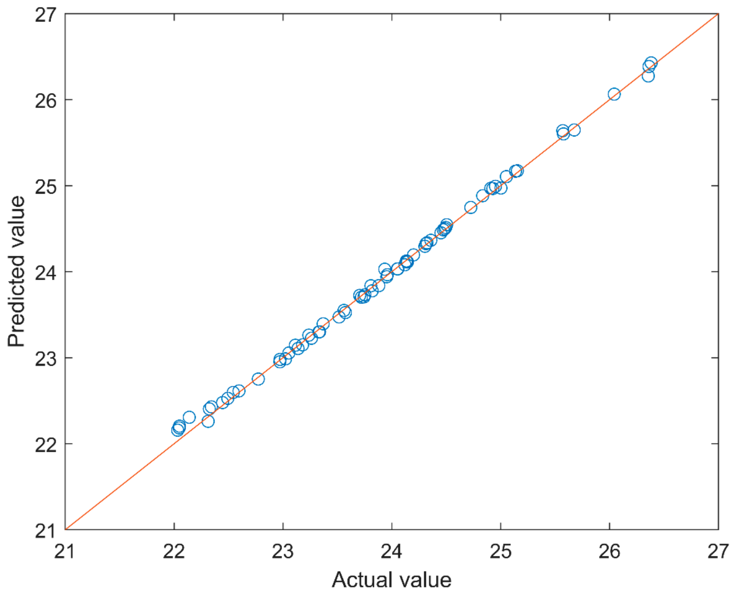

Figure 11. Comparison of predicted values and actual production values.

6. Conclusions

(1) Based on the data from the actual hourly production process of a steel enterprise's #2 blast furnace in June and July, outliers were detected using the isolated forest algorithm with the raw data, and the detected outliers are analyzed, eliminated, and/or retained. The hourly level data-driven samples were obtained through data deviation normalization, which can accurately predict the blast furnace permeability index after an hour to ensure the stable, smooth running of the blast furnace. Through the analysis of the coupling mechanism of blast furnace permeability and gas flow, Spearman correlation analysis, and MIC analysis of the selection of 25 key parameters affecting the production of the blast furnace, 14 characteristic variables were ultimately selected. These were: the roof pressure, the volume fraction of gas CO, the amount of coal spraying, the pressure difference, the volume fraction of gas CO_2, the furnace belly gas index, the utilization of the gas, the hot air pressure, the temperature of the top of the furnace, the amount of oxygen enrichment, the oxygen enrichment rate, the kinetic energy of the blowing air, the air temperature, and the flow rate of the cold air.

(2) The wavelet neural network (WNN) has a large advantage over a BP neural network (BP), a particle swarm-optimized BP neural network (PSO-BP), and Xgboost in the data-driven prediction of the blast furnace permeability index. The RMES (root mean square error), MAE (mean absolute error), and MAPE (mean absolute percentage error) with the model accuracy (error at ± 0.1) indicators are better than the other three models, and the model prediction accuracy reached 95.71% at an error of ± 0.1, which offers a great impact on blast furnace production compliance.

(3) Making full use of the data collected during the actual production of the blast furnace, we carried out the data-driven construction of a predictive model of the blast furnace permeability index and put the constructed model into the actual production of a No. 2 blast furnace of an iron and steel enterprise. The results showed that the predicted value of the blast furnace permeability index is very much in line with the actual value of real-time blast furnace production and maintains excellent characteristics. The aim of this study was to develop an efficient and reliable gas permeability index prediction model for blast furnaces to ensure the stable operation of the blast furnace smelting process. Therefore, it has considerable application prospects and a popularization value in actual blast furnace production.

Author Contributions: Conceptualization, K.T. and Z.L.; methodology, K.T.; software, K.T. and Z.L.; validation, K.T., Z.L. and Y.H.; formal analysis, K.T.; investigation, K.T.; resources, Y.H.; data curation, K.T.; writing—original draft preparation, K.T.; writing—review and editing, K.T.; visualization, K.T.; supervision, Z.L., Y.H., W.W. and X.Q.; project administration, K.T.; funding acquisition, Y.H. All authors have read and agreed to the published version of the manuscript.

Funding: This research was funded by the National Natural Science Foundation of China (No. 52074126); Tangshan Science and Technology Program (No. 22130201G); Natural Science Research Program of Higher Education Institutions in Hebei Province (No. QN2023153) and the Natural Science Foundation of Hebei Province (E2022209110).

Data Availability Statement: Not applicable.

Acknowledgments: Thanks are given to the Hebei Engineering Research Center for the Intelligentization of Iron Ore Optimization and Ironmaking Raw Materials Preparation Processes for their help with training. Special thanks to Aimin Yang for his meticulous guidance. We would also like to extend our appreciation to our colleagues for their unwavering support and companionship. Additionally, we would like to thank Zezheng Li, Zhenghan Xu, and Zhibin Hu for their valuable contributions to the manuscript.

Conflicts of Interest: The authors declare no conflict of interest.

References

1. Wang, S.; Li, Q. Combined big data and neural network for blast furnace permeability forecasting model. *Iron Steel* **2023**, *28*, 46–53.
2. Zheng, P. Experimental analysis of permeability of blast furnace lumpy zone. *China Metall.* **2020**, *30*, 10–14.
3. Cui, Z.; Han, Y.; Yang, A. Intelligent prediction of silicon content in hot metal of blast furnace based on neural network time series model. *Metall. Autom.* **2021**, *45*, 51–57.
4. Wang, X.; Jin, Y. Strategy analysis and testing study of high ratio of pellet utilized in blast furnace. *Iron Steel* **2021**, *56*, 7.
5. Han, Y.; Han, W. Improved Multidomain Convolutional Neural Network for Intelligent Tracking of Marangoni Effect Process Sequence Images. *IEEE Trans. Ind. Inform.* **2022**, *18*, 3397–3405. [CrossRef]
6. Zeb, A.; Din, F. A Systematic Literature Review on Robust Swarm Intelligence Algorithms in Search-Based Software Engineering. *Complexity* **2023**, *2023*, 4577581. [CrossRef]
7. Kumar, V.; Chowdhury, S. Hot Metal Silicon Prediction in a Blast Furnace by Using a Deep Neural Network. *Trans. Indian Inst. Met.* **2022**, *75*, 2009–2017. [CrossRef]
8. Spirin, N.A.; Polinov, A.A.; Gurin, I.A. Information system for real-time prediction of the silicon content of iron in a blast furnace. *Metallurgist* **2020**, *63*, 898–905. [CrossRef]
9. Azadi, P.; Winz, J.; Leo, E. A hybrid dynamic model for the prediction of molten iron and slag quality indices of a large-scale blast furnace. *Comput. Chem. Eng.* **2022**, *156*, 107573. [CrossRef]
10. Nag, S.; Gupta, A.; Paul, S. Prediction of heap shape in blast furnace burden distribution. *ISIJ Int.* **2014**, *54*, 1517–1520. [CrossRef]
11. Su, X.; Zhang, S.; Yin, Y. Prediction model of permeability index for blast furnace based on the improved multi-layer extreme learning machine and wavelet transform. *J. Frankl. Inst.* **2018**, *355*, 1663–1691. [CrossRef]
12. Qian, C.; Tian, Y. An introduction to the methods and suggestions for handling outliers. In Proceedings of the China Metrology Association Metallurgy Branch Smelting Sensor Specialized Committee 2013 Annual Meeting and Technical Exchange Conference, Yichang, China, 13–14 September 2013; pp. 139–140.
13. Li, Z.; Chu, M.; Liu, Z.; Li, B. Prediction and optimization of blast furnace parameters based on machine learning and genetic algorithm. *J. Northeast. Univ.* **2020**, *41*, 1262–1267.
14. Sun, R.; Wei, L. Data cleaning of wind power anomalies based on isolated forest and standard deviation detection method. *Henan Sci.* **2023**, *41*, 313–320.
15. Lvanov, E.; Klimovitskii, M.; Anisimov, E. Expert system for blast-furnace operators. *Metallurgist* **2011**, *54*, 730–736.
16. Guo, Y.; Zhang, H.; Chen, C. Discussion on reasonable blast kinetic energy of large blast furnace. *Ironmaking* **2016**, *35*, 18–23.
17. Pan, Y.; Jiang, Y.; Luo, D. Current status of research on factors influencing blast furnace permeability. *Jiangxi Metall.* **2022**, *42*, 22–30.
18. Li, Z.; Li, Y. Study on the Basic Characteristics of Iron Ore Powder with Different Particle Sizes. *Minerals* **2022**, *12*, 973. [CrossRef]
19. Yang, H.; Zhang, C.; Wang, L. Industrial IoT for Intelligent Steelmaking with Converter Mouth Flame Spectrum Information Processed by Deep Learning. *IEEE Trans. Ind. Inform.* **2020**, *16*, 2640–2650.
20. Xu, Y.J.; She, X.F.; Li, H.B. Simulation of gas flow distribution in blast furnace under different column modes. *China Metall.* **2023**, *33*, 54–61.
21. Shi, L.; Wen, Y.; Zhao, G. Recognition of blast furnace gas flow center distribution based on infrared image processing. *Iron Steel Res. Int.* **2016**, *23*, 203–209. [CrossRef]

22. Liu, H.; Ning, X.; Wang, Z. Simulation of gas flow velocity and pressure field under central coking system of blast furnace. *China Metall.* **2022**, *32*, 46–51.
23. Zhang, C.; Zhang, Y.; Yang, H. Industrial cyber-physical system driven intelligent prediction model for converter end carbon content in steelmaking plants. *J. Ind. Inf. Integr.* **2022**, *28*, 100356. [CrossRef]
24. Zhang, H.; Liu, L. Shougang No.2 blast furnace charging system adjustment practice. *Ironmaking* **2005**, *24*, 12.
25. Cheng, H. Short-term load forecasting based on BP neural network. *Fujian Qual. Manag.* **2019**, *016*, 256–258.
26. Lin, Z.Y.; Zhen, Z.K.; Yin, S. Application and research of wavelet neural network based on particle swarm algorithm. *Mod. Surv. Mapp.* **2011**, *34*, 6–8.
27. Tan, Y.L.; Saffari, S.E.; Tan, N. A framework for evaluating predictive models. *J. Clin. Epidemiol.* **2022**, *150*, 188–190. [CrossRef]